The ups and downs of brain stress: Extending the triple network hypothesis

Gina-Isabelle Henze[1,2,3,4,*], Marina Giglberger[4], Christoph Bärtl[1,2,4], Julian Konzok[4,5], Maja Neidhart[1,2,6], Tabea Krause[1], Emin Serin[1,2], Lea Waller[1,2], Hannah L. Peter[4], Ludwig Kreuzpointner[4], Nina Speicher[4], Fabian Streit[7,8,9], Ilya M. Veer[1,10], Peter Kirsch[9,11], Thomas E. Nichols[3,12], Brigitte M. Kudielka[4], Stefan Wüst[4], Susanne Erk[1,2] & Henrik Walter[1,2]

[1]Research Division of Mind and Brain, Department of Psychiatry and Psychotherapy CCM, Charité-Universitätsmedizin Berlin, Corporate Member of Freie Universität Berlin, Humboldt-Universität zu Berlin, and Berlin Institute of Health, Berlin, Germany

[2]German Center for Mental Health (DZPG), Partner Site Berlin - Potsdam, Germany

[3]Big Data Institute, Li Ka Shing Centre for Health Information and Discovery, Nuffield Department of Population Health, University of Oxford, Oxford, United Kingdom

[4]Institute of Psychology, University of Regensburg, Regensburg, Germany

[5]Department of Epidemiology and Preventive Medicine, University of Regensburg, Regensburg, Germany

[6]Department of Child and Adolescent Psychiatry and Psychotherapy, Central Institute of Mental Health, Medical Faculty Mannheim, University of Heidelberg, Mannheim, Germany

[7]Hector Institute for Artificial Intelligence in Psychiatry, Central Institute of Mental Health, Medical Faculty Mannheim, Heidelberg University, Mannheim, Germany

[8]Department of Psychiatry and Psychotherapy, Central Institute of Mental Health, Medical Faculty Mannheim, Heidelberg University, Mannheim, Germany

[9]German Center for Mental Health (DZPG), Partner Site Mannheim - Heidelberg - Ulm, Germany

[10]Department of Developmental Psychology, University of Amsterdam, Amsterdam, Netherlands

[11]Department of Clinical Psychology, Central Institute of Mental Health, Medical Faculty Mannheim, University of Heidelberg, Heidelberg, Germany

[12]Wellcome Centre for Integrative Neuroimaging, FMRIB, Nuffield Department of Clinical Neurosciences, University of Oxford, Oxford, United Kingdom

*Corresponding author email: gina-isabelle.henze@charite.de

Supplemental Material

SUPPLEMENTAL BACKGROUND

Table S1. Overview of all Scan*STRESS* and Montreal Imaging Stress Task (MIST) studies including sample size for imaging analysis (*N*); sex ratio (women/men/non-binary; w/m/n); information on female subjects regarding menstrual cycle phase, contraception (OC), and reproductive status; paradigm version (OV, original version; SV, shortened version; MV, modified version); as well as information on the stress induction categorised by cortisol, negative affect, and heart rate response to the stressor (↑, increase; ↔, unchanged; ↓, decrease). For negative affect ratings, we considered different measures (e.g., negative affect, stress, bad mood, state anxiety, current distress).

	Sample			Stress response		
Studies	***N* (w/m/n)**	**Women: menstrual cycle phase, contraception, reproductive status**	**Paradigm version**	**Cortisol**	**Negative Affect**	**Heart rate**
Scan*STRESS* studies						
Akdeniz et al.[1]; Streit et al[2]	80 (41/39/0)	n/a	OV	↑	↑	↑
Bärtl et al.[3]	106 (56/59/0)	13 OCs, 25 luteal, 18 post-menopause	OV	↑	↑	↑
Chand et al.[4]	39 (0/39/0)	-	SV	↔	↑	↑
Dahm et al.[5]; Dimitrov et al.[6]	86 (50/36/0)	23 OCs, 27 luteal	OV	↑	↑	
Giglberger et al.[7]	111 (70/41/0)	56 OCs, 14 luteal	OV	↑		
Henze et al.[8–11]	67 (31/36/0)	OCs	OV	↑	↑	↑
Hermann et al.[12]; Nanni-Zapeda et al.[13]	36 (0/36/0)	-	SV			
Hu et al.[14]; Li et al.[15]	70 (31/39/0)	luteal	OV	↑	↑	
Konzok et al.[16]	61 (30/31/0)	15 OCs, 15 luteal	OV	↑	↑	↑
Kuhn et al.[17]	39 (0/39/0)	-	OV	↑	↑	
Kuhn et al.[18]	140 (67/73/0)	OCs	OV	↓	↑	↑
Lederbogen et al.[19]	57 (25/32/0)	n/a	OV	↑	↑	↑
Liu et al. [20] &	72 (32/40/0)					
Ren et al[21];	71 (31/40/0)					
Zhao et al.[22]	77 (35/42/0)	luteal	OV	↑	↑	
Nowak et al.[23] &	45 (0/45/0)					
Dimitrov et al.[24,25]	42 (0/42/0)	-	SV	↑	↑	↑
Sandner et al.[26]	40 (12/28/0)	OCs	Compact	↑	↑	↑
Sandner et al.[27]	40 (n/a)	n/a	Compact	↑	↑	↑
Speicher et al.[28]	40 (0/40/0)	-	OV	↑	↑	↑
Streit et al.[2,29]; Lederbogen et al.[30]	42 (20/22/0)	luteal	OV	↔		↑

MIST studies						
Ackermann et al.[31]	39 (23/16/0)	OCs	OV	↑	↑	
Albert et al.[32]	28 (28/0/0)	10 early follicular, 10 ovulation	OV	↑		
Albert et al.[33]	65 (65/0/0)	post-menopause	OV			
Allenby et al.[34]	75 (35/40/0)	n/a	MV	↔	↑	
Alpheis et al.[35]*	79 (28/51/0)	n/a	MV	↑ (n.s.)	↑	
Alyan et al.[36]	10 (0/10/0)	-	MV			
Alyan et al.[37]	23 (0/23/0)	-	MV			
Alyan et al.[38]	15 (0/15/0)	-	MV			
Ashare et al.[39]	39 (17/22/0)	n/a	OV		↑	
Baumeister et al.[40]	84 (62/22/0)	n/a	OV	↑	↑	
Bloomfield et al.[41]	34 (17/17/0)	n/a	MV	↑	↑	↑**
Boehringer et al.[30]	25 (14/11/0)					
Lederbogen et al.[30]	32 (16/16/0)	n/a	OV	↑	↑	↑
Brugnera et al.[42,43]	60 (31/29/0)	8 OCs	MV		↑	↑
Bürger et al.[44]	73 (40/43/0)	19 early follicular 2 ovulation, 19 midluteal	MV	↔	↑	
Choi[45]	37 (20/17/0)	n/a	MV			
Chung et al.[46]	31 (31/0/0)	15 early follicular, 16 midluteal	MV	↓	↑	
Chung et al.[47]	46 (30/16/0)	15 early follicular, 15 OCs	MV	↓	↑	
Cohen et al.[48]	42 (21/21/0)	early follicular	MV	↑	↑	
Corbett et al.[49]	78 (0/78/0)	-	OV	↓		
Corr et al.[50–52]	101 (44/57/0)	n/a	MV	↑	↑	↑
Dagher et al.[53]	15 (7/8/0)	n/a	OV	↔		
	53 (45/8/0)	31 OCs	OV	↓	↑	↑
De Calheiros Velozo et al.[54]	30 (27/3/0)	n/a	rMIST	↓	↑	↑
De Calheiros Velozo et al.[55]	53 (46/7/0)	n/a	MV			↑
De Wandel et al.[56]	60 (31/29/0)	OCs	MV		↑	
Dedovic et al.[57]	22 (0/22/0)	-	OV	↑		
Dedovic et al.[58]	28 (0/28/0)	-	eventMIST	↔		
Dedovic et al.[59]*	49 (25/24/0)	8 follicular, 2 luteal, 15 OCs	MV	↔	↔	
Degroote et al.[60]	56 (0/56/0)	-	OV	↑		
Dettweiler[61]	48 (20/28/0)	-	MV			
Dong et al.[62]	148 (85/63/0)	n/a	OV	↑	↑	
Dong et al.[63,64]	367 (213/154/0)	n/a	OV	↑	↑	
Edebol Carlman et al.[65]	22 (16/6/0)	n/a	OV	↔	↑	
Ethridge et al.[66]	100 (0/100/0)	-	MV	↑	↑	
Fan et al.[67]	18 (0/18/0)	-	OV	↑	↑	
Geva et al.[68]	29 (0/29/0)	-	MV	↑	↑	↑
Geva et al.[69]	25 (0/25/0)	-	MV	↑	↑	↑

Geva et al.[70]	148 (82/66/0)	n/a	MV	↑	↑	↑
Gheorghe et al.[71]	48 (27/21/0)	before exclusion N = 35 women: 17 follicular, 8 luteal, 1 amenorrhea, 9 OCs	MV	↔	↑	
Golde et al.[72]	46 (46/0/0)	10 OCs, 8 follicular, 23 luteal, 4 post-menopause, 1 n/a	MV	↑	↑	↑
Golde et al.[73]	41 (22/19/0)	n/a	MV		↑	↑
Goodman et al.[74]	51 (22/29/0)	n/a	MV			
Goodman et al.[75,76]	120 (67/53/0)	n/a	MV			
Goodman et al.[77]*	72 (55/17/0)	n/a	MV	↓		↑
Goodman et al.[78]	15 (6/9/0)	n/a	MV			↑
Goodman et al.[79]	84 (72/12/0)	n/a	MV			
Gossett et al.[70]	57 (21/36/0)	n/a	MV	↓		↑
Grimm et al.[80]	32 (0/32/0)	-	OV	↑		
Grodin et al.[81]*	25 (10/15/0)	n/a	OV		↔	
Guffanti et al.,[82]; Treadway et al.[83]	75 (75/0/0) 70 (70/0/0)	n/a	MV	↔	↑	
Hachtel et al.[70]	32 (0/32/0)	-	OV	↑	↑	
Hakimi et al.[84]	20 (0/20/0)	-	MV			
Hoegh et al.[85]	25 (0/25/0)	-	MV	↔	↑	
Inagaki et al.[70]	36 (16/20/0)	n/a	MV		↑	
Jones et al.[86]	22 (11/11/0)	n/a	MV	↑		↑
Joseph et al.[87]*	119 (50/69/0)	n/a	OV			
Khalili-Mahani et al.[88]	19 (0/19/0)	-	OV	↔		
Kim et al.[89]	18 (0/18/0)	-	OV			
Kirsch et al.[90,91]*	42 (30/12/0)	n/a	MV			↑
Kogler et al.[92,93]*	43 (23/20/0)	11 OCs	MV	↔	↑	
Kogler et al.[94]	80 (40/40/0)	20 mid-luteal, 20 early follicular	MV	↓	↑	
König et al.[95]	62 (n/a/0)	n/a	MV		↑	
La Marca et al.[96]	43 (0/43/0)	-	OV	↑	↑	↑
Leicht-Deobald et al.[97]	31 (14/17/0)	n/a	OV			↑
Li et al.[98]	140 (71/69/0)	natural cycling	OV	↑	↑	
Lord et al.[99]*	39 (39/0/0)	postpartum	MV	↔	↑	
Luo et al.[100]	44 (23/21/0)	luteal	OV	↑	↑	
Ming et al.[101]*	105 (54/51/0)	n/a	OV	↑	↑	
Minguillon et al.[102]	6 (n/a)	-	MV			↑
Murray et al.[103]	47 (27/20/0)	n/a	MV			↑
Murray et al.[104]*	73 (50/23/0)	n/a	MV			↑
Nair et al.[105]	32 (21/11/0)	n/a	MV			↔
Nair et al.[106]	36 (24/12/0)	n/a	MV			↔
Nathan et al.[107]*	37 (37/0/0)	peri- & post-menopause	OV			

Nitschke et al.[108]	46 (26/20/0)	natural cycling	OV	↑		
Orem et al.[109]	239 (113/126/0)	n/a	MV	↓	↑	↑
Perez-Valero et al.[110]	23 (14/9/0)	n/a	MV			
Pruessner et al.[111]	39 (16/23/0)	n/a	OV			
Pruessner et al.[112]; Lederbogen et al.[30]	40 (20/20/0)	OCs	OV	↑		
Raufelder et al.[113]	41 (22/19/0)	n/a	MV			
Ren et al.[114]	44 (23/11/0)	luteal	OV	↑	↑	
Ren et al.[115]	53 (0/53/0)	-	MV	↑	↑	
Richer et al.[116]	25 (20/5/0)	n/a	MV	↑	↑	↑
Richter et al.[117]	31 (16/15/0)	n/a	OV	↔	↑	↑
Rojas-Thomas et al.[118]	62 (0/62/0)	-	MV	↑	↑	↑
Saraf et al.[119]*	20 (6/14/0)	OCs, pre-menopause	MV	↔		↔
Schifani et al.[120]	33 (14/19/0)	n/a	MV		↑	
Shakra et al.[121]	35 (14/21/0)	n/a	OV		↑	
Shermohammed et al.[70]	54 (27/27/0)	n/a	MV	↑	↑	↑
Sigrist et al.[122]	27 (27/0/0)	OCs, natural cycling	OV			↑
Soliman et al.[123]*	40 (27/13/0)	natural cycling	OV		↑	
Sun et al.[124]	307 (153/154/0)	n/a	OV	↑	↑	
Sun et al.[125]	101 (0/101/0)	-	OV	↑	↑	
Tomova et al.[126]	67 (0/67/0)	-	MV	↑	↑	
Vaessen et al.[127]*	29 (13/16/0)	n/a	MV		↑	
Vaquero-Blasco et al.[128]	20 (n/a)	n/a	MV		↑	
Vaquero-Blasco et al.[129]	23 (14/8/1)	n/a	MV		↑	
Voellmin et al.[130]	104 (104/0/0)	OCs, luteal	OV	↑	↑	↑
Voges et al.[131]	65 (39/26/0)	n/a	OV	↔	↔	
Wheelock et al.[132]	53 (23/30/0)	n/a	eventMIST	↔	↑	↑
Yamaoka et al.[133]	59 (0/59/0)	-	MV		↑	↑
Zhang et al.[134]	115(62/53/0)	n/a	OV	↑	↑	
Zhao et al.[135]	51 (0/51/0)	-	MV		↑	↑**
Zhong et al.[136]	96 (57/39/0)	n/a	OV	↑	↑	
Zhukovsky et al.[137]*	115 (n/a)	follicular	MV	↑		
Zschucke et al.[138]	36 (0/36/0)	-	MV		↑	

Note. *Studies including (pre-)clinical samples; n.s., not significant; **Increase in BP, Blood Pressure; rMIST, repeated Montreal Imaging Stress Task.

SUPPLEMENTAL RESULTS

Figure S1. Comparison of whole-brain responses for the total sample (corrected for *age*, *sex*, and *site*) with (A) four sites (Regensburg, Mannheim, Berlin 1, and Berlin 2; $z_{FDR} > 3.77$) and with (B) three sites, excluding Berlin 2 ($z_{FDR} > 3.82$).

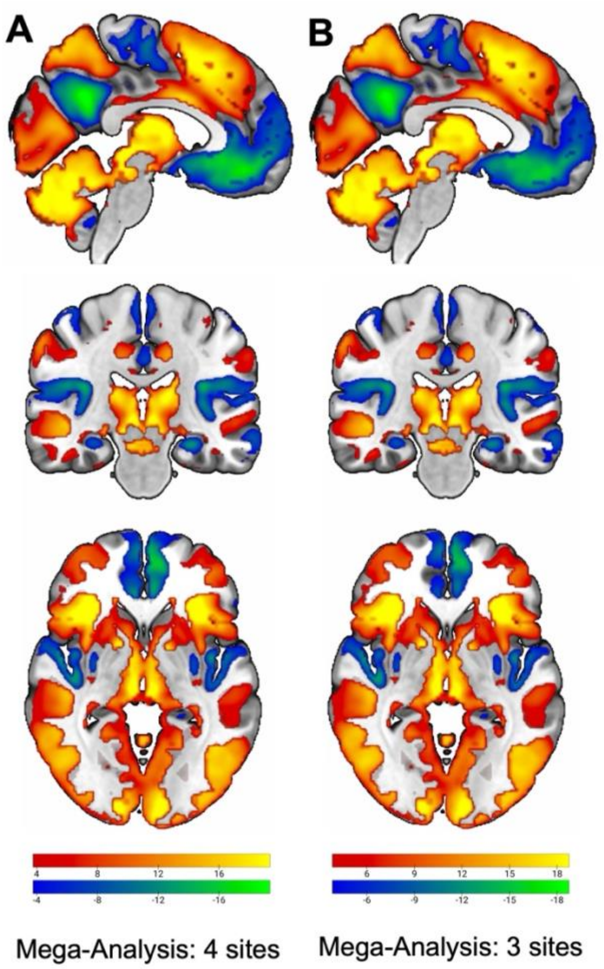

Table S2. One-sample *t*-test results: Activated ($stress > control$) and deactivated ($control > stress$) structures during psychosocial stress for the total sample (corrected for *age*, *sex*, and *site*) including cluster size *k*, individual *z*-values, localisation of peak voxels (voxel and Montréal Neurological Institute, MNI coordinates), as well as hemisphere-specific structure labelling (L-R, left-right) and network-integration. False-discovery rate (FDR, $p < .05$) correction at $z_{FDR} > 3.77$.

			Voxel coordinates			MNI coordinates					
Cluster	***k***	***z***	**X**	**Y**	**Z**	**X**	**Y**	**Z**	**Structure**		**Network**
1	90511	24.90	46	53	36	-4.50	-26.50	-6.50		Brain stem	
2	60	8.43	40	51	68	-16.50	-30.50	57.50	L	Precentral gyrus	Motor
3	22533	-19.50	29	57	49	-38.50	-18.50	19.50	L	Central opercular cortex	SN
4	3716	-21.00	44	40	55	-8.50	-52.50	31.50	L	Posterior cingulate cortex	DMN
5	1104	-19.60	23	33	55	-50.50	-66.50	31.50	L	Lateral occipital cortex	Visual
6	625	-15.60	77	34	57	57.50	-64.50	35.50	R	Lateral occipital cortex	Visual
7	91	-9.38	67	84	32	37.50	35.50	-14.50	R	Frontal pole	CEN
8	51	-6.33	20	80	40	-56.50	27.50	1.50	L	Inferior frontal gyrus	Speech

Note. SN, Salience Network; DMN, Default Mode Network.

Table S3. One-sample t-test results: Activated ($stress > control$) and deactivated ($control > stress$) structures during psychosocial stress for the Regensburg site (corrected for *age* and *sex*) including cluster size k, individual z-values, localisation of peak voxels (voxel and Montréal Neurological Institute, MNI coordinates), as well as hemisphere-specific structure labelling (L-R, left-right) and network-integration. False-discovery rate (FDR, $p < .05$) correction at $z_{FDR} > 3.45$.

			Voxel coordinates			MNI coordinates					
Cluster	***k***	***z***	**X**	**Y**	**Z**	**X**	**Y**	**Z**	**Structure**		**Network**
1	86839	20.80	64	80	39	31.50	27.50	-0.50	R	Orbitofrontal cortex	SN
2	19208	-16.60	28	57	48	-40.50	-18.50	17.50	L	Central opercular cortex	SN
3	4147	-15.90	67	58	49	37.50	-16.50	19.50	R	Central opercular cortex	SN
4	4119	-17.30	45	39	53	-6.50	-54.50	27.50	L	Posterior cingulatex cortex	DMN
5	1039	-16.10	24	33	55	-48.50	-66.50	31.50	L	Lateral occipital cortex	Visual
6	571	-12.70	77	35	57	57.50	-62.50	35.50	R	Lateral occipital cortex	Visual
7	222	-5.59	56	93	60	15.50	53.50	41.50	R	Frontal pole	CEN
8	57	-7.62	68	85	31	39.50	37.50	-16.50	R	Frontal pole	CEN
9	32	-5.28	19	79	43	-58.50	25.50	7.50	L	Inferior frontal gyrus	Speech

Note. SN, Salience Network; DMN, Default Mode Network; CEN, Central Executive Network.

Table S4. One-sample *t*-test results: Activated ($stress > control$) and deactivated ($control > stress$) structures during psychosocial stress for the Mannheim site (corrected for *age* and *sex*) including cluster size *k*, individual *z*-values, localisation of peak voxels (voxel and Montréal Neurological Institute, MNI coordinates), as well as hemisphere-specific structure labelling (L-R, left-right) and network-integration. False-discovery rate (FDR, $p < .05$) correction at $z_{FDR} > 3.53$.

			Voxel coordinates			**MNI coordinates**					
Cluster	***k***	***z***	**X**	**Y**	**Z**	**X**	**Y**	**Z**	**Structure**		**Network**
1	68145	9.13	46	53	36	-4.50	-26.50	-6.50		Brain stem	
2	208	6.18	61	96	33	25.50	59.50	-12.50	R	Frontal pole	CEN
3	165	6.76	49	53	52	1.50	-26.50	25.50	R	Posterior cingulate cortex	DMN
4	39	4.49	18	53	41	-60.50	-26.50	3.50	L	Planum temporale	Auditory
5	23	4.92	57	53	68	17.50	-26.50	57.50	R	Precentral gyrus	Motor
6	19	4.65	31	48	47	-34.50	-36.50	15.50	L	Planum temporale	Auditory
7	2684	-7.18	45	85	31	-6.50	37.50	-16.50	L	Medial prefrontal cortex	DMN
8	941	-7.59	44	39	55	-8.50	-54.50	31.50	L	Posterior cingulate cortex	DMN
9	558	-7.63	20	33	58	-56.50	-66.50	37.50	L	Lateral occipital cortex	Visual
10	304	-5.11	16	65	27	-64.50	-2.50	-24.50	L	Middle temporal gyrus	SN
11	148	-5.58	68	60	48	39.50	-12.50	17.50	R	Central opercular cortex	SN
12	135	-5.77	76	32	56	55.50	-68.50	33.50	R	Lateral occipital cortex	Visual
13	88	-5.62	65	78	20	33.50	23.50	-38.50	R	Temporal pole	SN
14	40	-4.81	35	57	30	-26.50	-18.50	-18.50	L	Hippocampus	DMN
15	34	-5.05	29	57	49	-38.50	-18.50	-18.50	L	Parahippocampus	DMN
16	30	-4.92	27	78	22	-42.50	23.50	-34.50	L	Temporal pole	SN
17	29	-4.55	42	96	57	-12.50	59.50	35.50	L	Frontal pole	CEN
18	20	-4.13	26	83	32	-44.50	33.50	-14.50	L	Orbitofrontal cortex	SN

Note. SN, Salience Network; DMN, Default Mode Network; CEN, Central Executive Network.

Table S5. One-sample *t*-test results: Activated ($stress > control$) and deactivated ($control > stress$) structures during psychosocial stress for the Berlin 1 site (corrected for *age* and *sex*) including cluster size *k*, individual *z*-values, localisation of peak voxels (voxel and Montréal Neurological Institute, MNI coordinates), as well as hemisphere-specific structure labelling (L-R, left-right) and network-integration. False-discovery rate (FDR, $p < .05$) correction at $z_{FDR} > 3.50$.

			Voxel coordinates			**MNI coordinates**					
Cluster	***k***	***z***	**X**	**Y**	**Z**	**X**	**Y**	**Z**	**Structure**		**Network**
1	63679	10.60	46	54	37	-4.50	-24.50	-4.50	L	Thalamus	SN
2	119	5.57	76	71	30	55.50	9.50	-18.50	R	Temporal pole	SN
3	92	5.50	35	55	68	-26.50	-22.50	57.50	L	Precentral gyrus	Motor
4	24	4.85	60	55	68	23.50	-22.50	57.50	L	Precentral gyrus	Motor
5	1292	-8.63	44	40	55	-8.50	-52.50	31.50	L	Posterior cingulate cortex	DMN
6	1040	-7.22	44	95	36	-8.50	57.50	-6.50	L	Frontal pole	CEN
7	755	-6.95	22	65	22	-52.50	-2.50	-34.50	L	Middle temporal gyrus	SN
8	737	-8.39	29	57	49	-38.50	-18.50	19.50	L	Central opercular cortex	SN
9	606	-7.63	67	58	49	37.50	-16.50	19.50	R	Central opercular cortex	SN
10	577	-8.48	23	32	58	-50.50	-68.50	37.50	L	Lateral occipital cortex	Visual
11	268	-7.13	76	35	58	55.50	-62.50	37.50	R	Lateral occipital cortex	Visual
12	142	-5.48	54	71	33	11.50	9.50	-12.50	R	Ncl. accumbens	SN
13	138	-6.46	41	72	34	-14.50	11.50	-10.50	R	Putamen	SN
14	102	-4.70	40	86	65	-16.50	39.50	51.50	L	Frontal pole	CEN
15	90	-5.44	35	56	31	-26.50	-20.50	-16.50	L	Hippocampus	DMN
16	74	-5.43	76	63	24	55.50	-6.50	-30.50	R	Middle temporal gyrus	SN
17	66	-4.93	36	77	29	-24.50	21.50	-20.50	L	Orbitofrontal cortex	SN
18	53	-5.22	58	67	22	19.50	1.50	-34.50	R	Parahippocampus	DMN
19	33	-5.25	45	95	59	-6.50	57.50	39.50	L	Frontal pole	CEN
20	25	-4.15	65	86	34	33.50	39.50	-10.50	R	Frontal pole	CEN

Note. SN, Salience Network; DMN, Default Mode Network; CEN, Central Executive Network.

Table S6. One-sample *t*-test results: Activated ($stress > control$) and deactivated ($control > stress$) structures during psychosocial stress for the Berlin 2 site (corrected for *age* and *sex*) including cluster size *k*, individual *z*-values, localisation of peak voxels (voxel and Montréal Neurological Institute, MNI coordinates), as well as hemisphere-specific structure labelling (L-R, left-right) and network-integration. False-discovery rate (FDR, $p < .05$) correction at $z_{FDR} > 3.85$.

			Voxel coordinates			MNI coordinates					
Cluster	***k***	***z***	**X**	**Y**	**Z**	**X**	**Y**	**Z**	**Structure**		**Network**
1	1804	7.40	41	61	44	-14.50	-10.50	9.50	L	Thalamus	SN
2	1156	6.73	27	83	49	-42.50	33.50	19.50	L	Middle frontal gyrus	CEN
3	689	5.65	69	85	51	41.50	37.50	23.50	R	Frontal pole	CEN
4	543	7.20	53	72	64	9.50	9.50	49.50	R	Paracingulate gyrus	DMN
5	535	7.21	37	64	63	-22.50	-4.50	47.50	L	Superior frontal gyrus	CEN
6	528	7.85	64	79	42	31.50	25.50	5.50	R	Insular cortex	SN
7	515	7.35	44	74	65	-8.50	15.50	51.50	L	Superior frontal gyrus	CEN
8	465	7.18	32	78	45	-32.50	23.50	11.50	L	Frontal opercular cortex	SN
9	395	6.54	65	65	65	33.50	-2.50	51.50	R	Middle frontal gyrus	CEN
10	357	5.79	71	71	51	45.40	9.50	23.50	R	Inferior frontal gyrus	Speech
11	41	5.62	57	53	59	17.50	-26.50	39.50	R	Precentral gyrus	Motor
12	29	5.29	50	72	53	3.50	11.50	27.50	R	Anterior cingulate cortex	SN
13	25	5.13	31	59	60	-34.50	-14.50	41.50	L	Precentral gyrus	Motor
14	23	5.72	63	92	32	29.50	51.50	-14.50	R	Frontal pole	CEN
15	3214	-7.96	53	87	37	9.50	41.50	-4.50	R	Paracingulate gyrus	DMN
16	1338	-7.00	26	72	22	-44.50	11.50	-34.50	L	Temporal pole	SN
17	665	-6.70	21	33	56	-54.50	-66.50	33.50	L	Lateral occipital cortex	Visual
18	411	-6.20	77	62	43	57.50	-8.50	7.50	R	Central opercular cortex	SN
19	409	-5.98	67	78	22	37.50	23.50	-34.50	R	Temporal pole	SN
20	246	-5.70	40	89	59	-16.50	45.50	39.50	L	Frontal pole	CEN
21	219	-6.54	64	62	28	31.50	-8.50	-22.50	R	Hippocampus	DMN
22	194	-6.75	63	83	33	29.50	33.50	-12.50	R	Frontal pole	CEN
23	182	-5.33	78	36	55	59.50	-60.50	31.50	R	Lateral occipital cortex	Visual
24	168	-6.08	55	78	39	13.50	23.50	-0.50	R	Ncl. caudatus	SN
25	66	-5.28	74	63	31	51.50	-6.50	-16.50	R	Superior temporal gyrus	SN

26	50	-5.65	68	74	28	39.50	15.50	-22.50	R	Temporal pole	SN
27	44	-5.22	47	52	70	-2.50	-28.50	61.50	L	Precentral gyrus	Motor
28	35	-4.94	30	55	49	-36.50	-22.50	19.50	L	Central opercular cortex	SN
29	29	-4.90	74	52	47	51.50	-28.50	15.50	R	Parietal opercular cortex	SN
30	27	-4.94	77	68	25	57.50	3.50	-28.50	R	Middle temporal gyrus	SN
31	26	-5.27	48	60	57	-0.50	-12.50	35.50	R	Anterior cingulate cortex	SN
32	20	-5.76	57	81	69	17.50	29.50	59.50	R	Superior frontal gyrus	CEN

Note. SN, Salience Network; DMN, Default Mode Network; CEN, Central Executive Network.

Figure S2. Two-sample unpaired *t*-test results ($men > women$) for the total sample (corrected for *age* and *site*; $z_{FDR} > 3.44$).

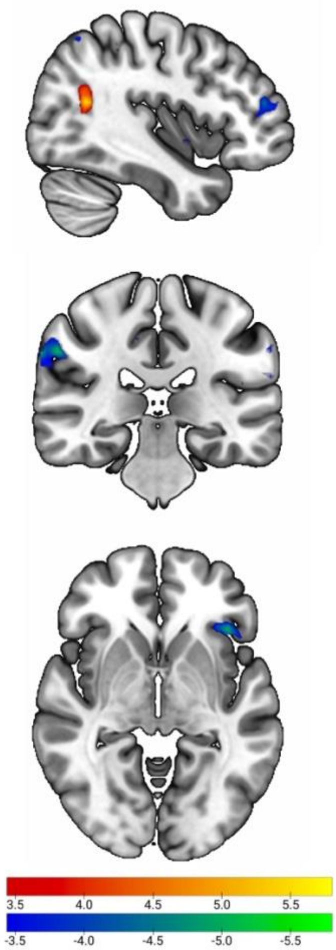

Table S7. Two-sample unpaired t-test results ($men > women$): Activated ($stress > control$) and deactivated ($control > stress$) structures during psychosocial stress for the total sample (corrected for *age* and *site*) including cluster size *k*, individual z-values, localisation of peak voxels (voxel and Montréal Neurological Institute, MNI coordinates), as well as hemisphere-specific structure labelling (L-R, left-right) and network-integration. False-discovery rate (FDR, $p < .05$) correction at $z_{FDR} > 3.44$.

			Voxel coordinates			MNI coordinates					
Cluster	***k***	***z***	**X**	**Y**	**Z**	**X**	**Y**	**Z**	**Structure**		**Network**
1	171	5.57	69	37	48	41.50	-58.50	17.50	R	Angular gyrus	DMN
2	284	-5.35	77	50	57	57.50	-32.50	35.50	R	Supramarginal gyrus	DMN
3	250	-4.97	66	93	48	35.50	53.50	17.50	R	Frontal pole	CEN
4	161	-5.03	28	79	38	-40.50	78.50	36.50	L	Frontal opercular cortex	SN
5	113	-5.33	56	46	66	15.50	-40.50	53.50	R	Postcentral gyrus	Motor
6	74	-4.51	43	26	63	-10.50	-80.50	47.50	L	Lateral occipital cortex	Visual
7	64	-4.86	55	25	63	13.50	-82.50	47.50	R	Lateral occipital cortex	Visual
8	42	-4.32	18	50	51	-60.50	-32.50	23.50	L	Parietal opercular cortex	SN
9	37	-4.50	55	54	59	13.50	-24.50	39.50	R	Posterior cingulate cortex	DMN
10	27	-4.18	18	45	55	-60.50	-42.50	31.50	L	Supramarginal gyrus	DMN
11	24	-5.09	27	89	53	-42.50	45.50	27.50	L	Frontal pole	CEN
12	22	-4.25	77	72	47	57.50	11.50	15.50	R	Inferior frontal gyrus	Speech
13	22	-4.51	30	91	44	-36.50	49.50	9.50	L	Frontal pole	CEN
14	22	-3.82	72	69	41	47.50	5.50	3.50	R	Central opercular cortex	SN
15	21	-3.99	72	80	35	47.50	27.50	-8.50	R	Orbitofrontal cortex	SN
16	21	-4.13	34	84	54	-38.50	35.50	29.50	R	Middle frontal gyrus	CEN

Note. SN, Salience Network; DMN, Default Mode Network; CEN, Central Executive Network.

Table S8. One-sample *t*-test with additional covariate (*age*) results: Activated ($stress > control$) structures during psychosocial stress for the total sample (corrected for *sex* and *site*) including cluster size *k*, individual *z*-values, localisation of peak voxels (voxel and Montréal Neurological Institute, MNI coordinates), as well as hemisphere-specific structure labelling (L-R, left-right) and network-integration. False-discovery rate (FDR, $p < .05$) correction at $z_{FDR} > 3.76$.

			Voxel coordinates			MNI coordinates					
Cluster	***k***	***z***	**X**	**Y**	**Z**	**X**	**Y**	**Z**	**Structure**		**Network**
1	2252	7.46	47	34	50	-2.50	-64.50	21.50	L	Precuneus cortex	DMN
2	1079	6.99	25	29	61	-46.50	-74.50	43.50	L	Lateral occipital cortex	Visual
3	730	6.04	44	92	35	-8.50	51.50	-8.50	L	Medial prefrontal cortex	DMN
4	714	6.03	77	36	58	57.50	-60.50	37.50	R	Lateral occipital cortex	Visual
5	343	5.15	37	83	64	-22.50	33.50	49.50	L	Superior frontal gyrus	CEN
6	237	5.42	16	50	38	-64.50	-32.50	-2.50	L	Middle temporal gyrus	SN
7	208	5.30	62	53	67	27.50	-26.50	55.50	R	Precentral gyrus	Motor
8	205	5.27	74	56	49	51.50	-20.50	19.50	R	Parietal opercular cortex	SN
9	196	5.73	50	91	31	3.50	49.50	-16.50	R	Medial prefrontal cortex	DMN
10	162	5.97	64	61	42	31.50	-10.50	5.50	R	Putamen	SN
11	85	5.57	41	51	73	-14.50	-30.50	67.50	L	Precentral gyrus	Motor
12	74	5.76	35	55	32	-26.50	-22.50	-14.50	L	Hippocampus	DMN
13	60	4.82	49	55	68	1.50	-22.50	57.50	R	Precentral gyrus	Motor
14	60	5.74	32	61	41	-32.50	-10.50	3.50	L	Putamen	SN
15	47	5.59	39	97	53	-18.50	61.50	27.50	L	Frontal pole	CEN
16	44	4.63	61	82	64	25.50	31.50	49.50	R	Superior frontal gyrus	CEN
17	44	4.56	23	81	34	-50.50	29.50	-10.50	L	Orbitofrontal cortex	SN
18	42	4.61	28	59	51	28.50	57.00	49.30	L	Central opercular cortex	SN
19	37	4.63	69	83	31	41.50	33.50	-16.50	R	Frontal pole	CEN
20	34	4.70	63	60	29	29.50	-12.50	-20.50	R	Hippocampus	DMN
21	33	4.75	52	49	67	7.50	-34.50	55.50	R	Postcentral gyrus	Motor
22	32	4.64	17	65	32	-62.50	-2.50	-14.50	L	Middle Temporal Gyrus	SN
23	31	5.18	36	48	31	-24.50	-36.50	-16.50	L	Parahippocampus	DMN
24	28	4.64	68	58	65	39.50	-16.50	51.50	R	Precentral gyrus	Motor
25	26	4.11	70	59	58	43.50	-14.50	37.50	R	Postcentral gyrus	Motor
26	25	5.00	75	83	38	53.50	33.50	-2.50	R	Frontal pole	CEN

27	24	4.37	66	63	22	35.50	-6.50	-34.50	R	Temporal fusiform cortex	Visual
28	24	5.00	46	60	58	-4.50	-12.50	37.50	L	Anterior cingulate cortex	SN
29	23	5.89	56	43	79	15.50	-46.50	79.50	R	Postcentral gyrus	Motor
30	23	6.15	41	44	79	-14.50	-44.50	79.50	L	Postcentral gyrus	Motor

Note. SN, Salience Network; DMN, Default Mode Network; CEN, Central Executive Network.

Figure S3. One-sample *t*-test with additional covariate (*age*) results: Comparison of whole-brain responses for the total sample (corrected for *sex* and *site*) including (A) all samples of all sites (Regensburg, Mannheim, Berlin 1, and Berlin 2; $z_{FDR} > 3.76$) and (B) omitting one sample from the Regensburg site (Bärtl et al.[3]; $z_{FDR} > 3.10$).

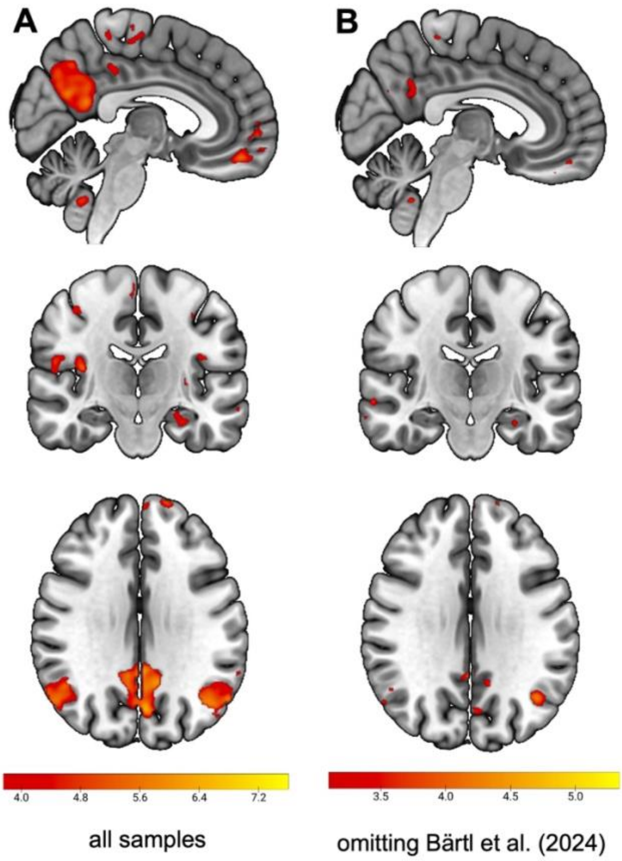

Table S9. Exposure-time effect results ($run\ 1 > run\ 2$): Structures showing more activations ($stress > control$) in the first run compared to the second run of Scan*STRESS* for the total sample (corrected for *age*, *sex*, and *site*) including cluster size *k*, individual *z*-values, localisation of peak voxels (voxel and Montréal Neurological Institute, MNI coordinates), as well as hemisphere-specific structure labelling (L-R, left-right) and network-integration. False-discovery rate (FDR, $p < .05$) correction at $z_{FDR} > 4.95$.

			Voxel coordinates			MNI coordinates					
Cluster	***k***	***z***	**X**	**Y**	**Z**	**X**	**Y**	**Z**	**Structure**		**Network**
1	55539	18.4	21	36	51	-54.50	-60.50	23.50	L	Angular gyrus	DMN
2	1514	15.1	61	26	21	25.50	-80.50	-36.50	R	Cerebellum	Motor
3	1106	14.5	36	26	21	-24.50	-80.50	-36.50	L	Cerebellum	Motor
4	620	12.2	51	40	18	5.50	-52.50	-42.50	R	Cerebellum	Motor
5	169	7.17	67	58	48	37.50	-16.50	17.50	R	Central opercular cortex	SN
6	119	7.14	68	59	58	39.50	-14.50	37.50	R	Precentral gyrus	Motor
7	36	6.78	29	57	59	-38.50	-18.50	39.50	L	Postcentral gyrus	Motor
8	31	6.02	30	56	48	-36.50	-20.50	17.50	L	Insular cortex	SN

Note. SN, Salience Network; DMN, Default Mode Network.

Table S10. One-sample *t*-test with additional covariate (*cortisol increase*) results: Activated ($stress > control$) structures during psychosocial stress for the total sample (corrected for *age*, *sex*, and *site*) including cluster size *k*, individual *z*-values, localisation of peak voxels (voxel and Montréal Neurological Institute, MNI coordinates), as well as hemisphere-specific structure labelling (L-R, left-right) and network-integration. False-discovery rate (FDR, $p < .05$) correction at $z_{FDR} > 2.54$.

			Voxel coordinates			MNI coordinates					
Cluster	***k***	***z***	**X**	**Y**	**Z**	**X**	**Y**	**Z**	**Structure**		**Network**
1	47	3.93	57	65	32	17.50	-2.50	-14.50	R	Amygdala	SN
2	26	4.18	67	64	34	37.50	-4.50	-10.50	R	Insular cortex	SN
3	25	3.11	76	44	52	55.50	-44.50	25.50	R	Angular gyrus	DMN
4	23	3.23	42	61	27	-12.50	-10.50	-24.50	L	Parahippocampus	DMN

Note. SN, Salience Network; DMN, Default Mode Network.

Figure S4. One-sample *t*-test with additional covariate (*cortisol*) results: Comparison of whole-brain responses ($stress > control$, $z_{FDR} > 2.54$) for the total sample (corrected for *age*, *sex*, and *site*) for peak voxel in the right amygdala for (A) cortisol increase (voxel coordinates: 57 65 32, $k = 47$), (B) AUCg (voxel coordinates: 55 65 33, $k = 18$), and (C) AUCi (voxel coordinates: 55 65 33, $k = 32$).

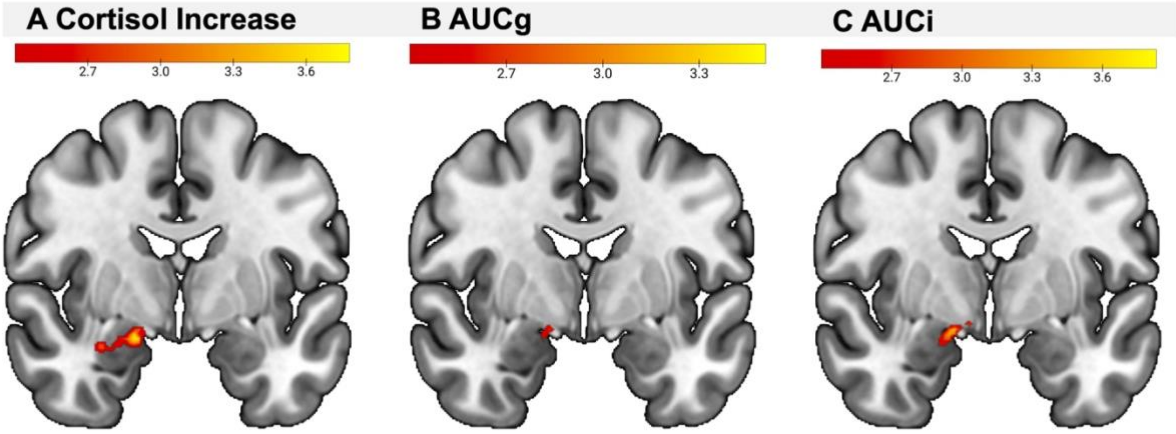

Table S11. Unpaired two-group ($men > women$) difference with continuous covariate interaction (*cortisol increase*) results: Activated ($stress > control$) structures during psychosocial stress for the total sample (corrected for *age* and *site*) including cluster size *k*, individual *z*-values, localisation of peak voxels (voxel and Montréal Neurological Institute, MNI coordinates), as well as hemisphere-specific structure labelling (L-R, left-right) and network-integration. False-discovery rate (FDR, $p < .05$) correction at $z_{FDR} > 2.94$.

			Voxel coordinates			**MNI coordinates**					
Cluster	***k***	***z***	**X**	**Y**	**Z**	**X**	**Y**	**Z**	**Structure**		**Network**
1	182	-5.18	69	64	36	41.50	-4.50	-6.50	R	Insular cortex	SN
2	173	-4.55	51	62	61	5.50	-8.50	43.50	R	Dorsal anterior cingulate cortex	SN
3	93	-4.18	44	74	42	-8.50	15.50	5.50	L	Ncl. caudatus	SN
4	48	-3.69	47	79	49	-2.50	25.50	19.50	L	Dorsal anterior cingulate cortex	SN
5	46	-3.56	40	51	42	-16.50	-30.50	5.50	L	Thalamus	SN
6	42	-3.56	60	65	31	23.50	-2.50	-16.50	R	Amygdala	SN
7	39	-3.81	35	56	24	-26.50	-20.50	-30.50	L	Parahippocampus	DMN
8	38	-3.70	50	91	35	3.50	49.50	-8.50	R	Medial prefrontal cortex	DMN
9	34	-3.94	45	46	55	-6.50	-40.50	31.50	L	Posterior cingulate cortex	DMN
10	30	-3.85	63	77	41	29.50	21.50	3.50	R	Insular cortex	SN
11	26	-4.21	30	57	39	-36.50	-18.50	-0.50	L	Insular cortex	SN

Note. SN, Salience Network; DMN, Default Mode Network.

Figure S5. Unpaired two-group ($men > women$) difference with continuous covariate interaction (*cortisol increase*) results: Comparison of whole-brain responses ($stress > control$, $z_{FDR} > 2.94$) for the total sample (corrected for *age*, *sex*, and *site*) for peak voxel in the right insula for (A) cortisol increase (voxel coordinates: 69 64 36, $k = 182$), (B) AUCg (voxel coordinates: 69 64 36, $k = 5$), and (C) AUCi (voxel coordinates: 69 64 36, $k = 18$).

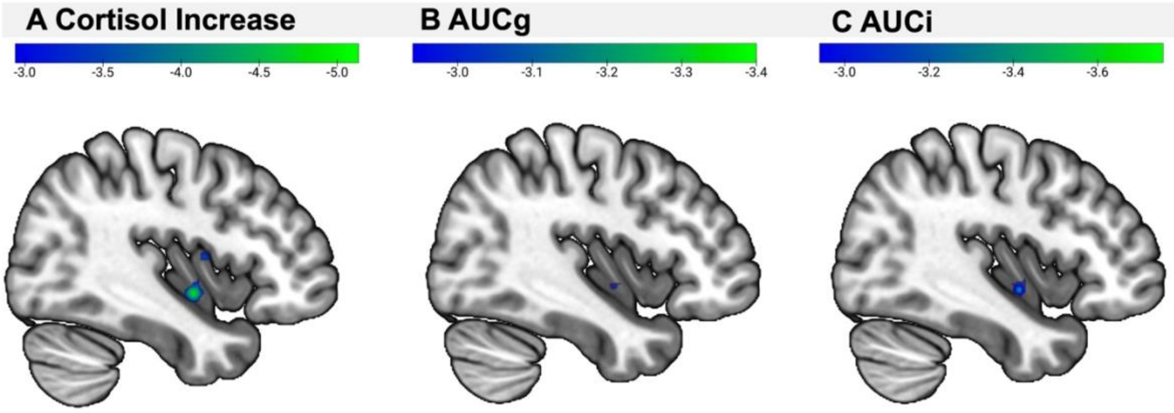

Table S12. One-sample *t*-test with additional covariate (*heart rate*) results: Activated ($stress > control$) structures during psychosocial stress for the total sample (corrected for *age*, *sex*, and *site*) including cluster size *k*, individual *z*-values, localisation of peak voxels (voxel and Montréal Neurological Institute, MNI coordinates), as well as hemisphere-specific structure labelling (L-R, left-right) and network-integration. False-discovery rate (FDR, $p < .05$) correction at $z_{FDR} > 3.1$.

			Voxel coordinates			MNI coordinates					
Cluster	***k***	***z***	**X**	**Y**	**Z**	**X**	**Y**	**Z**	**Structure**		**Network**
1	36	-3.74	48	50	54	-0.50	-32.50	29.50	L	Posterior cingulate cortex	DMN
2	35	-3.94	16	43	49	-64.50	-46.50	19.50	L	Supramarginal gyrus	DMN
3	33	-3.70	46	91	44	-4.50	49.50	9.50	L	Paracingulate gyrus	DMN
4	31	-4.08	38	63	21	-20.50	-6.50	-36.50	L	Parahippocampus	DMN

Note. DMN, Default Mode Network.

Table S13. One-sample *t*-test with additional covariate (*negative affect*) results: Activated ($stress > control$) structures during psychosocial stress for the total sample (corrected for *age*, *sex*, and *site*) including cluster size *k*, individual *z*-values, localisation of peak voxels (voxel and Montréal Neurological Institute, MNI coordinates), as well as hemisphere-specific structure labelling (L-R, left-right) and network-integration. False-discovery rate (FDR, $p < .05$) correction at $z_{FDR} > 2.77$.

			Voxel coordinates			MNI coordinates					
Cluster	***k***	***z***	**X**	**Y**	**Z**	**X**	**Y**	**Z**	**Structure**		**Network**
1	64	3.78	69	68	41	41.5	3.5	3.5	R	Insular cortex	SN
2	51	3.79	52	63	62	7.5	-6.5	45.5	R	Dorsal anterior cingulate cortex	SN
3	46	3.44	76	53	56	55.5	-26.5	33.5	R	Supramarginal gyrus	DMN

Note. SN, Salience Network; DMN, Default Mode Network.

Table S14. Unpaired two-group ($men > women$) difference with continuous covariate interaction (*negative affect*) results: Activated ($stress > control$) structures during psychosocial stress for the total sample (corrected for *age* and *site*) including cluster size *k*, individual *z*-values, localisation of peak voxels (voxel and Montréal Neurological Institute, MNI coordinates), as well as hemisphere-specific structure labelling (L-R, left-right) and network-integration. False-discovery rate (FDR, $p < .05$) correction at $z_{FDR} > 3.10$.

			Voxel coordinates			MNI coordinates					
Cluster	***k***	***z***	**X**	**Y**	**Z**	**X**	**Y**	**Z**	**Structure**		**Network**
1	41	-4.38	49	70	56	1.5	7.5	33.5	R	Dorsal anterior cingulate cortex	SN

Note. SN, Salience Network.

Table S15. One-sample *t*-test with additional covariate (*error rate*) results: Activated ($stress > control$) structures during psychosocial stress for the total sample (corrected for *age*, *sex*, and *site*) including cluster size *k*, individual *z*-values, localisation of peak voxels (voxel and Montréal Neurological Institute, MNI coordinates), as well as hemisphere-specific structure labelling (L-R, left-right) and network-integration. False-discovery rate (FDR, $p < .05$) correction at $z_{FDR} > 3.10$.

			Voxel coordinates			MNI coordinates					
Cluster	***k***	***z***	**X**	**Y**	**Z**	**X**	**Y**	**Z**	**Structure**		**Network**
1	31	4.2	49	77	31	1.5	21.5	-16.5	R	Subgenual anterior cingulate cortex	DMN
2	20	3.99	51	94	29	5.5	55.5	-20.5	R	Frontal pole	CEN

Note. DMN, Default Mode Network; CEN, Central Executive Network.

Table S16. Unpaired two-group ($men > women$) difference with continuous covariate interaction (*error rate*) results: Activated ($stress > control$) structures during psychosocial stress for the total sample (corrected for *age* and *site*) including cluster size *k*, individual *z*-values, localisation of peak voxels (voxel and Montréal Neurological Institute, MNI coordinates), as well as hemisphere-specific structure labelling (L-R, left-right) and network-integration. False-discovery rate (FDR, $p < .05$) correction at $z_{FDR} > 3.10$.

			Voxel coordinates			**MNI coordinates**					
Cluster	***k***	***z***	**X**	**Y**	**Z**	**X**	**Y**	**Z**	**Structure**		**Network**
1	29	3.84	51	94	29	5.5	55.5	-20.5	R	Frontal pole	CEN

Note. CEN, Central Executive Network.

Table S17. Generalized Psychophysiological Interaction (gPPI) results: Structures with increased/positive connectivity (PPI+) during psychosocial stress to seed regions of the triple network for the total sample (corrected for *age*, *sex*, and *site*) including localisation of peak voxels (Montréal Neurological Institute, MNI coordinates), hemisphere-specific structure labelling (L-R, left-right), and network-integration, as well as cluster size *k*, individual *z*-values, and Family-wise error ($p_{FWE} < .05$) correction at $z_{FWE} > 3.10$.

Seed	**MNI**								
	X	**Y**	**Z**	**Structure**		**Network**	**k**	***z***	p_{FWE}
SN: left FIC									
SN: right FIC	-26.5	27.5	-14.5	L	Orbitofrontal cortex	SN	149	4.15	.0003
	-46.5	33.5	-12.5	L	Frontal pole	CEN		4.08	
	-44.5	23.5	-20.5	L	Temporal pole	SN		3.93	
	-32.5	31.5	-18.5	L	Orbitofrontal cortex	SN		3.74	
	-46.5	31.5	-4.5	L	Inferior frontal gyrus	Speech		3.33	
	29.5	3.5	-20.5	R	Amygdala	SN	112	4.49	.0026
DMN: PCU/PCC	61.5	-40.5	33.5	R	Supramarginal gyrus	DMN	8591	8.59	.0001
	37.5	7.5	-4.5	R	Insular cortex	SN		7.41	
	53.5	13.5	-8.5	R	Temporal pole	SN		7.19	
	-62.5	-40.5	31.5	L	Supramarginal gyrus	DMN	5302	8.38	.0001
	-40.5	-10.5	-12.5	L	Planum polare	Auditory		7.59	
	-42.5	5.5	-6.5	L	Insular cortex	SN		7.24	
	-58.5	-32.5	21.5	L	Parietal opercular cortex	SN		6.61	
	3.5	-20.5	25.5	R	Middle cingulate cortex	SN	3578	7.17	.0001
	-4.5	9.5	29.5	L	Dorsal anterior cingulate cortex	SN		6.30	
	7.5	5.5	37.5	R	Dorsal anterior cingulate cortex	SN		6.21	
	-10.5	-32.5	41.5	L	Middle cingulate cortex	SN		5.99	
	-4.5	-88.5	21.5	L	Cuneal cortex	Visual	1252	5.22	.0001
	-12.5	-88.5	29.5	L	Occipital pole	Visual		5.19	
	5.5	-82.5	27.5	R	Cuneal cortex	Visual		4.98	
	-42.5	37.5	23.5	L	Dorsolateral prefrontal cortex	CEN	1018	6.52	.0001
	-38.5	43.5	23.5	L	Frontal pole	CEN		6.04	
	-28.5	35.5	19.5	L	Middle frontal gyrus	CEN		5.17	
	-30.5	43.5	-20.5	L	Frontal pole	CEN	173	5.66	.0001
	-26.5	35.5	-16.5	L	Orbitofrontal cortex	SN		4.89	

	25.5	39.5	-22.5	R	Frontal pole	CEN	144	4.66	.0005
	21.5	15.5	-6.5	R	Putamen	SN	104	4.56	.0045
CEN: left dlPFC	-36.5	37.5	-6.5	L	Frontal pole	CEN	204	4.62	.0001
	9.5	-34.5	5.5	R	Thalamus	SN	195	4.82	.0001
	27.5	-38.5	3.5	R	Hippocampus	DMN		4.42	
	35.5	-36.5	-16.5	R	Parahippocampus	DMN		4.36	
	37.5	-44.5	-14.5	R	Temporooccipital fusiform cortex	Visual		3.95	
	19.5	33.5	-10.5	R	Frontal pole	CEN	133	3.40	.0001
	19.5	9.5	17.5	R	Ncl. caudatus	SN	103	4.27	.0051
CEN: right rdlPFC	-54.5	19.5	9.5	L	Inferior frontal gyrus	Speech	581	4.91	.0001
	-46.5	41.5	-12.5	L	Frontal pole	CEN		4.22	
	-44.5	33.5	-8.5	L	Orbitofrontal cortex	SN		4.21	
	-6.5	29.5	-4.5	L	Subgenual anterior cingulate cortex	DMN	98	4.39	.0075
	-8.5	29.5	-10.5	L	Subcallosal cortex	DMN		3.72	
	-4.5	-14.5	-4.5	L	Thalamus	SN	88	4.70	.0134
	1.5	-12.5	-4.5	R	Thalamus	SN		4.37	

Note. SN, Salience Network; FIC, frontoinsular cortex; DMN, Default Mode Network; PCU/PCC, precuneus/posterior cingulate cortex; CEN, Central Executive Network, dlPFC, dorsolateral prefrontal cortex.

Table S18. Generalized Psychophysiological Interaction (gPPI) results: Structures with decreased/negative connectivity (PPI-) during psychosocial stress to seed regions of the triple network for the total sample (corrected for *age*, *sex*, and *site*) including localisation of peak voxels (Montréal Neurological Institute, MNI coordinates), hemisphere-specific structure labelling (L-R, left-right), and network-integration, as well as cluster size *k*, individual *z*-values, and Family-wise error ($p_{FWE} < .05$) correction at $z_{FWE} > 3.10$.

Seed		**MNI**							
	X	**Y**	**Z**	**Structure**		**Network**	**k**	***z***	***p*-FWE**
SN: left FIC	-52.5	-56.5	25.5	L	Angular gyrus	DMN	378	4.86	.0001
	-48.5	-68.5	35.5	R	Lateral occipital cortex	Visual		4.21	
	-56.5	-50.5	33.5	L	Supramarginal gyrus	DMN		3.84	
	-4.5	11.5	51.5	L	Paracingulate gyrus	DMN	292	4.54	.0001
	-4.5	-0.5	47.5	L	Supplementary motor cortex	Motor		3.35	
	-54.5	13.5	29.5	L	Inferior frontal gyrus	Speech	261	4.95	.0001
	-44.5	3.5	45.5	L	Middle frontal gyrus	CEN		4.94	
	-42.5	-0.5	33.5	L	Precentral gyrus	Motor		4.55	
	-60.5	-54.5	-10.5	L	Middle temporal gyrus	SN	90	4.08	.0096
	-6.5	47.5	45.5	L	Frontal pole	CEN	83	4.06	.0147
	-4.5	33.5	51.5	L	Superior frontal gyrus	CEN		3.71	
SN: right FIC	43.5	41.5	19.5	R	Frontal pole	CEN	1469	6.23	.0001
	11.5	-86.5	-0.5	R	Intracalcarine cortex	Visual	914	5.29	.0001
	-10.5	-78.5	7.5	L	Intracalcarine cortex	Visual		5.20	
	35.5	-04.5	-8.5	R	Occipital pole	Visual		4.68	
	5.5	29.5	25.5	R	Dorsal anterior cingulate cortex	SN	878	5.72	.0001
	-2.5	27.5	33.5	L	Paracingulate gyrus	DMN		5.64	
	3.5	33.5	35.5	R	Paracingulate gyrus	DMN		5.57	
	41.5	-48.5	43.5	R	Angular gyrus	DMN	639	6.46	.0001
	47.5	-44.5	33.5	R	Supramarginal gyrus	DMN		4.96	
	37.5	-58.5	43.5	R	Lateral occipital cortex	Visual		4.77	
	-30.5	43.5	27.5	L	Frontal pole	CEN	611	5.56	.0001
	-48.5	-48.5	39.5	L	Supramarginal gyrus	DMN	513	6.05	.0001
	-32.4	-58.5	33.5	L	Lateral occipital cortex	Visual		5.64	
	-50.5	-56.5	39.5	L	Angular gyrus	DMN		4.41	
	-46.5	-23.5	29.5	L	Postcentral gyrus	Motor	409	4.94	.0001

	-54.5	15.5	29.5	L	Inferior frontal gyrus	Speech		4.76	
	-50.5	29.5	21.5	L	Middle frontal gyrus	CEN		4.56	
	-50.5	5.5	33.5	L	Precentral gyrus	Motor		4.44	
	-60.5	-16.5	5.5	L	Planum temporale	Auditory	361	5.00	.0001
	-60.5	-2.5	23.5	L	Precentral gyrus	Motor		4.78	
	-66.5	-14.5	13.5	L	Postcentral gyrus	Motor		4.74	
	-52.5	-16.5	7.5	L	Heschl's gyrus	Auditory		4.19	
	59.5	-10.5	-0.5	R	Planum polare	Auditory	310	5.38	.0001
	49.5	-10.5	1.5	R	Heschl's gyrus	Auditory		3.94	
	57.5	-6.5	-15.5	R	Middle temporal gyrus	SN	219	4.76	.0001
	59.5	-2.5	25.5	R	Precentral gyrus	Motor		4.16	
	55.5	-8.5		R	Postcentral gyrus	Motor		3.90	
	39.5	9.5	-6.5	R	Insular cortex	SN	218	5.06	.0001
	49.5	17.5	-8.5	R	Temporal pole	SN		4.60	
	51.5	11.5	25.5	R	Inferior frontal gyrus	Speech	197	4.78	.0001
	15.5	3.5	13.5	R	Ncl. caudatus	SN	163	4.73	.0001
	15.5	9.5	-4.5	R	Putamen	SN		3.31	
	-18.5	5.5	7.5	L	Putamen	SN	151	4.32	.0003
	-8.5	7.5	9.5	L	Ncl. caudatus	SN		3.60	
	-42.5	-22.5	47.5	L	Postcentral gyrus	Motor	141	4.68	.0005
	63.5	-22.5	-8.5	R	Middle temporal gyrus	SN	134	4.85	.0008
DMN: PCU/PCC	-12.5	-52.5	1.5	L	Lingual gyrus	Visual	1314	6.47	.0001
	21.5	19.5	43.5	R	Superior frontal gyrus	CEN	519	5.72	.0001
	25.5	27.5	47.5	R	Middle frontal gyrus	CEN		5.69	
	3.5	-20.5	25.5	R	Lateral occipital cortex	Visual	495	7.07	.0001
	-42.5	-78.5	33.5	L	Lateral occipital cortex	Visual	478	9.12	.0001
	-30.5	9.5	49.5	L	Middle frontal gyrus	CEN	375	5.47	.0001
	-24.5	23.5	37.5	L	Superior frontal gyrus	CEN		4.99	
	-0.5	51.5	-18.5	L	Medial prefrontal cortex	DMN	350	6.98	.0001
	-0.5	55.5	-16.5	L	Frontal pole	CEN		6.89	
	63.5	-8.5	-20.5	R	Middle temporal gyrus	SN	130	5.25	.0010
CEN: left ldlPFC	57.5	-38.5	45.5	R	Supramarginal gyrus	DMN	5992	7.26	.0001

	31.5	-52.5	39.5	R	Superior parietal lobule	CEN		6.37	
	-60.5	-42.5	41.5	L	Supramarginal gyrus	DMN	3788	8.46	.0001
	-60.5	-68.5	-2.5	L	Lateral occipital cortex	Visual		6.31	
	-62.5	-56.5	-6.5	L	Middle temporal gyrus	SN		5.79	
	-4.5	-31.5	23.5	L	Posterior cingulate cortex	DMN	1929	5.91	.0001
	3.5	-22.5	41.5	R	Posterior cingulate cortex	DMN		5.37	
	-0.5	-42.5	45.5	L	Precuneus	DMN		5.35	
	45.5	11.5	-8.5	R	Insular cortex	SN	893	6.94	.0001
	49.5	17.5	-12.5	R	Temporal pole	SN		6.03	
	55.5	13.5	1.5	R	Inferior frontal gyrus	Speech		5.54	
	-42.5	-20.5	45.5	L	Postcentral gyrus	Motor	272	5.03	.0001
	-0.5	15.5	31.5	L	Dorsal anterior cingulate cortex	SN	262	5.25	.0001
	7.5	9.5	35.5	R	Anterior cingulate cortex	SN		3.93	
	-46.5	45.5	9.5	L	Frontal pole	CEN	232	4.51	.0001
	-48.5	13.5	-10.5	L	Temporal pole	SN	130	5.24	.0012
	1.5	-94.5	13.5	R	Occipital pole	Visual	83	4.50	.0165
	-0.5	-72.5	9.5	L	Intracalcarine cortex	Visual		4.05	
	1.5	-82.5	15.5	R	Supracalcarine cortex	Visual		3.69	
CEN: right rdlPFC	35.5	-58.5	43.5	R	Lateral occipital cortex	Visual	2490	6.97	.0001
	33.5	-52.5	37.5	R	Angular gyrus	DMN		6.77	
	3.5	-76.5	35.5	R	Cuneal cortex	Visual	1838	5.97	.0001
	7.5	-70.5	39.5	R	Precuneus	DMN		5.80	
	13.5	-48.5	33.5	R	Posterior cingulate cortex	DMN		5.36	
	-0.5	-44.5	43.5	L	Precuneus	DMN		4.85	
	-38.5	-60.5	39.5	L	Lateral occipital cortex	Visual	994	5.59	.0001
	-40.5	-50.5	43.5	L	Supramarginal gyrus	DMN		5.10	
	41.5	5.5	49.5	R	Middle Frontal gyrus	CEN	780	5.61	.0001
	55.5	-10.5	37.5	R	Postcentral gyrus	Motor		4.94	
	-54.5	-14.5	49.5	L	Postcentral gyrus	Motor	561	5.58	.0001
	-60.5	-4.5	33.5	L	Precentral gyrus	Motor		4.47	
	45.5	13.5	-8.5	R	Insular cortex	SN	254	5.26	.0001
	53.5	17.5	-10.5	R	Temporal pole	SN		4.64	

41.5	19.5	-6.5	R	Orbitofrontal cortex	SN		4.49	
45.5	35.5	27.5	R	Frontal pole	CEN	136	4.19	.0001
49.5	33.5	19.5	R	Middle frontal gyrus	CEN		3.89	
51.5	27.5	21.5	R	Inferior frontal gyrus	Speech		3.29	
-4.5	-10.5	53.5	L	Supplementary Motor cortex	Motor	131	4.19	.00125

Note. SN, Salience Network; FIC, frontoinsular cortex; DMN, Default Mode Network; PCU/PCC, precuneus/posterior cingulate cortex; CEN, Central Executive Network, dlPFC, dorsolateral prefrontal cortex.

REFERENCES

1. Akdeniz, C. *et al.* Neuroimaging evidence for a role of neural social stress processing in ethnic minority-associated environmental risk. *JAMA Psychiatry* **71**, 672–680 (2014).
2. Streit, F. *et al.* Sex-specific association between functional neuropeptide S receptor gene (NPSR1) variants and cortisol and central stress responses. *Psychoneuroendocrinology* **76**, 49–56 (2017).
3. Bärtl, C. *et al.* Neural and cortisol responses to acute psychosocial stress in work-related burnout: The Regensburg Burnout Project. *Psychoneuroendocrinology* **161**, 106926 (2023).
4. Chand, T. *et al.* Heart rate variability as an index of differential brain dynamics at rest and after acute stress induction. *Front. Neurosci.* **14**, 645 (2020).
5. Dahm, A. S. *et al.* The burden of conscientiousness? Examining brain activation and cortisol response during social evaluative stress. *Psychoneuroendocrinology* **78**, 48–56 (2017).
6. Dimitrov, A. *et al.* Differences in neural recovery from acute stress between cortisol responders and non-responders. *Front. Psychiatry* **9**, 631 (2018).
7. Giglberger, M. *et al.* Neural responses to acute stress predict chronic stress perception in daily life over 13 months. *Sci. Rep.* **13**, 19990 (2023).
8. Henze, G.-I. *et al.* Increasing deactivation of limbic structures over psychosocial stress exposure time. *Biol. Psychiatry Cogn. Neurosci. Neuroimaging* **5**, 697–704 (2020).
9. Henze, G.-I. *et al.* Sex-specific interaction between cortisol and striato-limbic responses to psychosocial stress. *Soc. Cogn. Affect. Neurosci.* **16**, 972–984 (2021).
10. Henze, G.-I. *et al.* Associations between cortisol stress responses and limbic volume and thickness in young adults: An exploratory study. *Eur. J. Neurosci.* **58**, 3962–3980 (2023).
11. Henze, G.-I. *et al.* Comparing two psychosocial stress paradigms for imaging environments – Scan*STRESS* and fNIRS-TSST: Correlation structures between stress responses. *Behav. Brain Res.* **436**, 114080 (2023).
12. Herrmann, L. *et al.* Nx4 attenuated stress-induced activity of the anterior cingulate cortex-A post-hoc analysis of a randomized placebo-controlled crossover trial. *Hum. Psychopharmacol.* **37**, e2837 (2022).
13. Nanni-Zepeda, M. *et al.* Trait anxiety is related to Nx4's efficacy on stress-induced changes in amygdala-centered resting state functional connectivity: A placebo-controlled cross-over trial in mildly to moderately stressed healthy volunteers. *BMC Neurosci.* **23**, 68 (2022).
14. Hu, W. *et al.* Reward sensitivity modulates the brain reward pathway in stress resilience via the inherent neuroendocrine system. *Neurobiol. Stress* **20**, 100485 (2022).
15. Li, Y. *et al.* Progressively decreased functional coupling within task positive networks during acute stress signals stress resilience: The promotion role of reward system. Preprint at https://doi.org/10.22541/au.167410577.75579496/v1 (2023).
16. Konzok, J. *et al.* Externalizing behavior in healthy young adults is associated with lower cortisol responses to acute stress and altered neural activation in the dorsal striatum. *Psychophysiology* **58**, e13936 (2021).
17. Kuhn, L. *et al.* The association of the 5-HTTLPR polymorphism and the response to different stressors in healthy males. *J. Neural Transm.* **128**, 1347–1359 (2021).
18. Kuhn, L. *et al.* Sex-dependent multimodal response profiles to psychosocial stress. *Cereb. Cortex* **33**, 583–596 (2023).
19. Lederbogen, F. *et al.* No association between cardiometabolic risk and neural reactivity to acute psychosocial stress. *NeuroImage Clin.* **20**, 1115–1122 (2018).
20. Liu, Y. *et al.* Neural habituation during acute stress signals a blunted endocrine response and poor resilience. *Psychol. Med.* **53**, 7735–7745 (2023).
21. Ren, Y. *et al.* Hair cortisone predicts lower stress-induced salivary cortisol response: Resting-state functional connectivity between salience and limbic networks. *Neuroscience* **517**, 61–69 (2023).
22. Zhao, X. *et al.* Separating the influences of means and daily variations of sleep on the stress-induced salivary cortisol response. *Psychoneuroendocrinology* **151**, 106059 (2023).
23. Nowak, J. *et al.* Association of naturally occurring sleep loss with reduced amygdala resting-state functional connectivity following psychosocial stress. *Psychoneuroendocrinology* **114**, 104585 (2020).

24. Dimitrov-Discher, A. *et al.* Residential green space and air pollution are associated with brain activation in a social-stress paradigm. *Sci. Rep.* **12**, 10614 (2022).
25. Dimitrov-Discher, A. *et al.* Stress and streets: How the network structure of streets is associated with stress-related brain activation. *J. Environ. Psychol.* **91**, 102142 (2023).
26. Sandner, M. *et al.* Investigating individual stress reactivity: High hair cortisol predicts lower acute stress responses. *Psychoneuroendocrinology* **118**, 104660 (2020).
27. Sandner, M., Zeier, P., Lois, G. & Wessa, M. Cognitive emotion regulation withstands the stress test: An fMRI study on the effect of acute stress on distraction and reappraisal. *Neuropsychologia* **157**, 107876 (2021).
28. Speicher, N. *et al.* Neural correlates of everyday moral decision-making: An exploratory ScanSTRESS study. *Psychol. Neurosci.* **16**, 71–95 (2023).
29. Streit, F. *et al.* A functional variant in the neuropeptide S receptor 1 gene moderates the influence of urban upbringing on stress processing in the amygdala. *Stress* **17**, 352–361 (2014).
30. Lederbogen, F. *et al.* City living and urban upbringing affect neural social stress processing in humans. *Nature* **474**, 498–501 (2011).
31. Ackermann, S., Cordi, M., La Marca, R., Seifritz, E. & Rasch, B. Psychosocial stress before a nap increases sleep latency and decreases early slow-wave activity. *Front. Psychol.* **10**, 20 (2019).
32. Albert, K., Pruessner, J. & Newhouse, P. Estradiol levels modulate brain activity and negative responses to psychosocial stress across the menstrual cycle. *Psychoneuroendocrinology* **59**, 14–24 (2015).
33. Albert, K., Ledet, T., Taylor, W. & Newhouse, P. Estradiol administration differentially affects the response to experimental psychosocial stress in post-menopausal women with or without a history of major depression. *J. Affect. Disord.* **261**, 204–210 (2020).
34. Allenby, C. *et al.* Brain marker links stress and nicotine abstinence. *Nicotine Tob. Res.* **22**, 885–891 (2020).
35. Alpheis, S. *et al.* Stress in musicians with and without focal dystonia is not reflected in limbic circuit activation. *Mov. Disord.* **39**, 2075–2086 (2024).
36. Alyan, E., Saad, N. M. & Kamel, N. Effects of workstation type on mental stress: FNIRS study. *Hum. Factors* **63**, 1230–1255 (2021).
37. Alyan, E., Saad, N. M., Kamel, N. & Rahman, M. A. Workplace design-related stress effects on prefrontal cortex connectivity and neurovascular coupling. *Appl. Ergon.* **96**, 103497 (2021).
38. Alyan, E. *et al.* Frontal electroencephalogram alpha asymmetry during mental stress related to workplace noise. *Sensors* **21**, 1968 (2021).
39. Ashare, R. L. *et al.* Nicotine withdrawal alters neural responses to psychosocial stress. *Psychopharmacology (Berl.)* **233**, 2459–2467 (2016).
40. Baumeister, D., Peters, E., Pruessner, J., Howes, O. & Chadwick, P. The effects of voice content on stress reactivity: A simulation paradigm of auditory verbal hallucinations. *Schizophr. Res.* **243**, 225–231 (2022).
41. Bloomfield, M. A., McCutcheon, R. A., Kempton, M., Freeman, T. P. & Howes, O. The effects of psychosocial stress on dopaminergic function and the acute stress response. *eLife* **8**, e46797 (2019).
42. Brugnera, A. *et al.* Cortical and cardiovascular responses to acute stressors and their relations with psychological distress. *Int. J. Psychophysiol.* **114**, 38–46 (2017).
43. Brugnera, A. *et al.* Heart rate variability during acute psychosocial stress: A randomized cross-over trial of verbal and non-verbal laboratory stressors. *Int. J. Psychophysiol. Off. J. Int. Organ. Psychophysiol.* **127**, 17–25 (2018).
44. Bürger, Z. *et al.* Stressor-specific sex differences in amygdala-frontal cortex networks. *J. Clin. Med.* **12**, 865 (2023).
45. Choi, M.-H. A pilot study: Extraction of a neural network and feature extraction of generation and reduction mechanisms due to acute stress. *Brain Sci.* **13**, 519 (2023).
46. Chung, K. C. *et al.* The influence of menstrual cycle and androstadienone on female stress reactions: An fMRI study. *Front. Hum. Neurosci.* **10**, 44 (2016).
47. Chung, K. C. *et al.* The influence of androstadienone during psychosocial stress is modulated by gender, trait anxiety, and subjective stress: An fMRI study. *Psychoneuroendocrinology* **68**, 126–139 (2016).

48. Cohen, J. E. *et al.* Neural response to stress differs by sex in young adulthood. *Psychiatry Res. Neuroimaging* **332**, 111646 (2023).
49. Corbett, B., Weinberg, L. & Duarte, A. The effect of mild acute stress during memory consolidation on emotional recognition memory. *Neurobiol. Learn. Mem.* **145**, 34–44 (2017).
50. Corr, R. *et al.* Neural mechanisms of acute stress and trait anxiety in adolescents. *NeuroImage Clin.* **29**, 102543 (2021).
51. Corr, R. *et al.* Stress-related hippocampus activation mediates the association between polyvictimization and trait anxiety in adolescents. *Soc. Cogn. Affect. Neurosci.* **17**, 767–776 (2022).
52. Corr, R. *et al.* Triple network functional connectivity during acute stress in adolescents and the influence of polyvictimization. *Biol. Psychiatry Cogn. Neurosci. Neuroimaging* **7**, 867–875 (2022).
53. Dagher, A., Tannenbaum, B., Hayashi, T., Pruessner, J. C. & McBride, D. An acute psychosocial stress enhances the neural response to smoking cues. *Brain Res.* **1293**, 40–48 (2009).
54. De Calheiros Velozo, J. *et al.* The repeated Montreal Imaging Stress Test (rMIST): Testing habituation, sensitization, and anticipation effects to repeated stress induction. *Psychoneuroendocrinology* **128**, 105217 (2021).
55. De Calheiros Velozo, J., Vaessen, T., Lafit, G., Claes, S. & Myin-Germeys, I. Is daily-life stress reactivity a measure of stress recovery? An investigation of laboratory and daily-life stress. *Stress Health* **39**, 638–650 (2023).
56. De Wandel, L. *et al.* The effects of left dorsolateral prefrontal transcranial direct current stimulation on episodic future thinking following acute psychosocial stress. *Memory* **31**, 380–392 (2023).
57. Dedovic, K. *et al.* The Montreal Imaging Stress Task: Using functional imaging to investigate the effects of perceiving and processing psychosocial stress in the human brain. *J. Psychiatry Neurosci.* **30**, 319–325 (2005).
58. Dedovic, K. *et al.* Neural correlates of processing stressful information: An event-related fMRI study. *Brain Res.* **1293**, 49–60 (2009).
59. Dedovic, K. *et al.* Psychological, endocrine, and neural responses to social evaluation in subclinical depression. *Soc. Cogn. Affect. Neurosci.* **9**, 1632–1644 (2014).
60. Degroote, C. *et al.* Acute stress-induced blood lipid reactivity in hypertensive and normotensive men and prospective associations with future cardiovascular risk. *J. Clin. Med.* **10**, 3400 (2021).
61. Dettweiler, U., Gerchen, M., Mall, C., Simon, P. & Kirsch, P. Choice matters: Pupils' stress regulation, brain development and brain function in an outdoor education project. *Br. J. Educ. Psychol.* **93**, 152–173 (2023).
62. Dong, D. *et al.* Neuroticism modulates neural activities of posterior cingulate cortex and thalamus during psychosocial stress processing. *J. Affect. Disord.* **262**, 223–228 (2020).
63. Dong, D. *et al.* Distinct stress-related medial prefrontal cortex activation in women with depression with and without childhood maltreatment. *Depress. Anxiety* **39**, 296–306 (2022).
64. Dong, D. *et al.* Sex-specific neural responses to acute psychosocial stress in depression. *Transl. Psychiatry* **12**, 1–8 (2022).
65. Edebol Carlman, H. M. T. *et al.* Probiotic mixture containing lactobacillus helveticus, bifidobacterium longum and lactiplantibacillus plantarum affects brain responses to an arithmetic stress task in healthy subjects: A randomised clinical trial and proof-of-concept study. *Nutrients* **14**, 1329 (2022).
66. Ethridge, P., Ali, N., Racine, S. E., Pruessner, J. C. & Weinberg, A. Risk and resilience in an acute stress paradigm: Evidence from salivary cortisol and time-frequency analysis of the reward positivity. *Clin. Psychol. Sci.* **8**, 872–889 (2020).
67. Fan, Y. *et al.* Early life stress modulates amygdala-prefrontal functional connectivity: Implications for oxytocin effects. *Hum. Brain Mapp.* **35**, 5328–5339 (2014).
68. Geva, N., Pruessner, J. & Defrin, R. Acute psychosocial stress reduces pain modulation capabilities in healthy men. *Pain* **155**, 2418–2425 (2014).
69. Geva, N., Pruessner, J. & Defrin, R. Triathletes lose their advantageous pain modulation under acute psychosocial stress. *Med. Sci. Sports Exerc.* **49**, 333–341 (2017).
70. Gossett, E. W. *et al.* Anticipatory stress associated with functional magnetic resonance imaging: Implications for psychosocial stress research. *Int. J. Psychophysiol.* **125**, 35–41 (2018).

71. Gheorghe, D. A., Panouillères, M. T. N. & Walsh, N. D. Psychosocial stress affects the acquisition of cerebellar-dependent sensorimotor adaptation. *Psychoneuroendocrinology* **92**, 41–49 (2018).
72. Golde, S. *et al.* Healthy women with severe early life trauma show altered neural facilitation of emotion inhibition under acute stress. *Psychol. Med.* **50**, 2075–2084 (2020).
73. Golde, S. *et al.* Adolescents' neural reactivity to acute psychosocial stress: Dysfunctional regulation habits are linked to temporal gyrus response. *Dev. Psychopathol.* **35**, 332–344 (2023).
74. Goodman, A. M. *et al.* The hippocampal response to psychosocial stress varies with salivary uric acid level. *Neuroscience* **339**, 396–401 (2016).
75. Goodman, A. M. *et al.* Anticipatory prefrontal cortex activity underlies stress-induced changes in Pavlovian fear conditioning. *NeuroImage* **174**, 237–247 (2018).
76. Goodman, A. M. *et al.* Stress-Induced Changes in Effective Connectivity During Regulation of the Emotional Response to Threat. *Brain Connect.* **12**, 629–638 (2022).
77. Goodman, A. M. *et al.* Neural response to stress and perceived stress differ in patients with left temporal lobe epilepsy. *Hum. Brain Mapp.* **40**, 3415–3430 (2019).
78. Goodman, A. M. *et al.* Repeatability of neural and autonomic responses to acute psychosocial stress. *Front. Neurosci.* **14**, 585509 (2020).
79. Goodman, A. M. *et al.* Altered fronto-limbic-motor response to stress differs between functional and epileptic seizures in a TBI model. *Epilepsy Behav.* **157**, 109877 (2024).
80. Grimm, S. *et al.* Early life stress modulates oxytocin effects on limbic system during acute psychosocial stress. *Soc. Cogn. Affect. Neurosci.* **9**, 1828–1835 (2014).
81. Grodin, E. N., Kirsch, D., Belnap, M. & Ray, L. A. Sex differences in neural response to an acute stressor in individuals with an alcohol use disorder. *Alcohol Clin. Exp. Res.* **48**, 843–854 (2024).
82. Guffanti, G. *et al.* Depression genetic risk score is associated with anhedonia-related markers across units of analysis. *Transl. Psychiatry* **9**, 236 (2019).
83. Treadway, M. T. *et al.* Association between interleukin-6 and striatal prediction-error signals following acute stress in healthy female participants. *Biol. Psychiatry* **82**, 570–577 (2017).
84. Hakimi, N., Jodeiri, A., Mirbagheri, M. & Setarehdan, S. K. Proposing a convolutional neural network for stress assessment by means of derived heart rate from functional near infrared spectroscopy. *Comput. Biol. Med.* **121**, 103810 (2020).
85. Hoegh, M., Poulsen, J. N., Petrini, L. & Graven-Nielsen, T. The effect of stress on repeated painful stimuli with and without painful conditioning. *Pain Med.* **21**, 317–325 (2020).
86. Jones, A. *et al.* Detailed assessment of the hemodynamic response to psychosocial stress using real-time MRI. *J. Magn. Reson. Imaging* **33**, 448–454 (2011).
87. Joseph, J. E. *et al.* Oxytocin moderates corticolimbic social stress reactivity in cocaine use disorder and healthy controls. *Compr. Psychoneuroendocrinology* **11**, 100150 (2022).
88. Khalili-Mahani, N., Dedovic, K., Engert, V., Pruessner, M. & Pruessner, J. C. Hippocampal activation during a cognitive task is associated with subsequent neuroendocrine and cognitive responses to psychological stress. *Hippocampus* **20**, 323–334 (2010).
89. Kim, D.-Y. *et al.* Electronic Cigarette Vaping Did Not Enhance the Neural Process of Working Memory for Regular Cigarette Smokers. *Front. Hum. Neurosci.* **16**, 817538 (2022).
90. Kirsch, D. E. *et al.* Neural functional connectivity changes to psychosocial stress in young adults with bipolar disorder and preliminary associations with clinical trajectories. *Bipolar Disord.* **24**, 298–309 (2022).
91. Le, V. *et al.* Recent perceived stress, amygdala reactivity to acute psychosocial stress, and alcohol and cannabis use in adolescents and young adults with bipolar disorder. *Front. Psychiatry* **12**, 767309 (2021).
92. Kogler, L., Gur, R. C. & Derntl, B. Sex differences in cognitive regulation of psychosocial achievement stress: brain and behavior. *Hum. Brain Mapp.* **36**, 1028–1042 (2015).
93. Kogler, L. *et al.* Cognitive stress regulation in schizophrenia patients and healthy individuals: Brain and behavior. *J. Clin. Med.* **12**, 2749 (2023).
94. Kogler, L. *et al.* Impact of self-esteem and sex on stress reactions. *Sci. Rep.* **7**, 17210 (2017).
95. König, M. *et al.* The stress-buffering role of friendships in young people with childhood threat experiences: A preliminary report. *Eur. J. Psychotraumatology* **14**, 2281971 (2023).
96. La Marca, R. *et al.* Association between Cold Face Test-induced vagal inhibition and cortisol response to acute stress. *Psychophysiology* **48**, 420–429 (2011).

97. Leicht-Deobald, U. *et al.* Work-related social support modulates effects of early life stress on limbic reactivity during stress. *Brain Imaging Behav.* **12**, 1405–1418 (2018).
98. Li, C. *et al.* Effect of corticotropin-releasing hormone receptor1 gene variation on psychosocial stress reaction via the dorsal anterior cingulate cortex in healthy adults. *Brain Res.* **1707**, 1–7 (2019).
99. Lord, C., Steiner, M., Soares, C. N., Carew, C. L. & Hall, G. B. Stress response in postpartum women with and without obsessive-compulsive symptoms: An fMRI study. *J. Psychiatry Neurosci.* **37**, 78–86 (2012).
100. Luo, J. *et al.* Role of hippocampus and orbitofrontal cortex in the association of interdependent self-construal with an acute stress response. *Neuropsychologia* **188**, 108620 (2023).
101. Ming, Q. *et al.* State-independent and dependent neural responses to psychosocial stress in current and remitted depression. *Am. J. Psychiatry* **174**, 971–979 (2017).
102. Minguillon, J., Lopez-Gordo, M. A. & Pelayo, F. Stress assessment by prefrontal relative gamma. *Front. Comput. Neurosci.* **10**, 101 (2016).
103. Murray, R. J. *et al.* Maladaptive emotion regulation traits predict altered corticolimbic recovery from psychosocial stress. *J. Affect. Disord.* **280**, 54–63 (2021).
104. Murray, R. J. *et al.* Identifying disease-specific neural reactivity to psychosocial stress in borderline personality disorder. *Biol. Psychiatry Cogn. Neurosci. Neuroimaging* **7**, 1137–1148 (2022).
105. Nair, N. *et al.* Effects of stress on functional connectivity during problem solving. *NeuroImage* **208**, 116407 (2020).
106. Nair, N. *et al.* Effects of stress on functional connectivity during verbal processing. *Brain Imaging Behav.* **14**, 2708–2723 (2020).
107. Nathan, M. D. *et al.* Hypothalamic-pituitary-adrenal axis, subjective, and thermal stress responses in midlife women with vasomotor symptoms. *Menopause* **28**, 439–443 (2020).
108. Nitschke, J. P., Giorgio, L.-M., Zaborowska, O. & Sheldon, S. Acute psychosocial stress during retrieval impairs pattern separation processes on an episodic memory task. *Stress* **23**, 437–443 (2020).
109. Orem, T. R. *et al.* Amygdala and prefrontal cortex activity varies with individual differences in the emotional response to psychosocial stress. *Behav. Neurosci.* **133**, 203–211 (2019).
110. Perez-Valero, E., Vaquero-Blasco, M. A., Lopez-Gordo, M. A. & Morillas, C. Quantitative assessment of stress through EEG during a virtual reality stress-relax session. *Front. Comput. Neurosci.* **15**, 684423 (2021).
111. Pruessner, J. C. *et al.* Self-esteem, locus of control, hippocampal volume, and cortisol regulation in young and old adulthood. *NeuroImage* **28**, 815–826 (2005).
112. Pruessner, J. C. *et al.* Deactivation of the limbic system during acute psychosocial stress: evidence from positron emission tomography and functional magnetic resonance imaging studies. *Biol. Psychiatry* **63**, 234–240 (2008).
113. Raufelder, D. *et al.* Adolescents' personality development - A question of psychosocial stress. *Front. Psychol.* **12**, 785610 (2021).
114. Ren, X. *et al.* The hippocampal-ventral medial prefrontal cortex neurocircuitry involvement in the association of daily life stress with acute perceived stress and cortisol responses. *Psychosom. Med.* **84**, 276–287 (2022).
115. Ren, J. *et al.* The interaction of oxytocin and nicotine addiction on psychosocial stress: An fMRI study. *Transl. Psychiatry* **14**, 348 (2024).
116. Richer, R., Zenkner, J., Küderle, A., Rohleder, N. & Eskofier, B. M. Vagus activation by Cold Face Test reduces acute psychosocial stress responses. *Sci. Rep.* **12**, 19270 (2022).
117. Richter, A. *et al.* Interaction of FKBP5 variant rs3800373 and city living alters the neural stress response in the anterior cingulate cortex. *Stress* **24**, 421–429 (2021).
118. Rojas-Thomas, F. *et al.* Impact of acute psychosocial stress on attentional control in humans. A study of evoked potentials and pupillary response. *Neurobiol. Stress* **25**, 100551 (2023).
119. Saraf, G. *et al.* Dopamine release during psychological stress in euthymic bipolar I disorder: a Positron Emission Tomography study with [11C]raclopride. *J. Affect. Disord.* **295**, 724–732 (2021).
120. Schifani, C. *et al.* Stress-induced cortical dopamine response is altered in subjects at clinical high risk for psychosis using cannabis. *Addict. Biol.* **25**, e12812 (2020).

121. Shakra, M. A. *et al.* Neurobiological correlates and predictors of two distinct personality trait pathways to escalated alcohol use. *eBioMedicine* **27**, 86–93 (2018).
122. Sigrist, C. *et al.* Cardiac autonomic functioning and clinical outcome in adolescent borderline personality disorder over two years. *Prog. Neuropsychopharmacol. Biol. Psychiatry* **111**, 110336 (2021).
123. Soliman, A. *et al.* Limbic response to psychosocial stress in schizotypy: A functional magnetic resonance imaging study. *Schizophr. Res.* **131**, 184–191 (2011).
124. Sun, X. *et al.* Influence of psychosocial stress on activation in human brain regions: Moderation by the 5-HTTLPR genetic locus. *Physiol. Behav.* **220**, 112876 (2020).
125. Sun, X. *et al.* The MAOA gene influences the neural response to psychosocial stress in the human brain. *Front. Behav. Neurosci.* **14**, 65 (2020).
126. Tomova, L. *et al.* Increased neural responses to empathy for pain might explain how acute stress increases prosociality. *Soc. Cogn. Affect. Neurosci.* **12**, 401–408 (2017).
127. Vaessen, T. *et al.* Neural correlates of daily-life affective stress reactivity in early psychosis: A study combining functional MRI and experience sampling methodology. *Schizophr. Res.* **255**, 93–101 (2023).
128. Vaquero-Blasco, M. A., Perez-Valero, E., Lopez-Gordo, M. A. & Morillas, C. Virtual reality as a portable alternative to chromotherapy rooms for stress relief: A preliminary study. *Sensors* **20**, 6211 (2020).
129. Vaquero-Blasco, M. A., Perez-Valero, E., Morillas, C. & Lopez-Gordo, M. A. Virtual reality customized 360-degree experiences for stress relief. *Sensors* **21**, 2219 (2021).
130. Voellmin, A. *et al.* Blunted endocrine and cardiovascular reactivity in young healthy women reporting a history of childhood adversity. *Psychoneuroendocrinology* **51**, 58–67 (2015).
131. Voges, J. F. *et al.* Association of stress-related neural activity and baseline interleukin-6 plasma levels in healthy adults. *Stress* **25**, 267–275 (2022).
132. Wheelock, M. D. *et al.* Prefrontal cortex activity is associated with biobehavioral components of the stress response. *Front. Hum. Neurosci.* **10**, 583 (2016).
133. Yamaoka, K., Uotsu, N. & Hoshino, E. Relationship between psychosocial stress-induced prefrontal cortex activity and gut microbiota in healthy Participants-A functional near-infrared spectroscopy study. *Neurobiol. Stress* **20**, 100479 (2022).
134. Zhang, D. *et al.* Neural mechanisms underlying the impact of psychological resilience on psychosocial stress responses. *Depress. Anxiety* **2024**, 5526584 (2024).
135. Zhao, W. *et al.* Impaired cognitive performance under psychosocial stress in cannabis-dependent men is associated with attenuated precuneus activity. *J. Psychiatry Neurosci.* **45**, 88–97 (2020).
136. Zhong, X. *et al.* Childhood maltreatment experience influences neural response to psychosocial stress in adults: An fMRI study. *Front. Psychol.* **10**, 2961 (2019).
137. Zhukovsky, P. *et al.* Acute stress increases striatal connectivity with cortical regions enriched for μ and κ opioid receptors. *Biol. Psychiatry* **96**, 717–726 (2024).
138. Zschucke, E., Renneberg, B., Dimeo, F., Wustenberg, T. & Strohle, A. The stress-buffering effect of acute exercise: evidence for HPA axis negative feedback. *Psychoneuroendocrinology* **51**, 414–425 (2015).